Climate Services 7 (2017) 64–77

Contents lists available at ScienceDirect

Climate Services

journal homepage: www.elsevier.com/locate/cliser

Impacts of 2°C global warming on primary production and soil carbon storage capacity at pan-European level

Abdulla Sakalli [a,b,*], Alessandro Cescatti [b], Alessandro Dosio [b], Mehmet Ugur Gücel [a]

[a] Iskenderun Technical University, Meydan Mah. 512 Sk., 31230, Iskenderun, Hatay, Turkey
[b] European Commission, Joint Research Centre (JRC), Via Enrico Fermi 2749, 21027, Ispra, Italy

ARTICLE INFO

Article history:
Available online 12 April 2017

Keywords:
Climate Change
Gross Primary Production
Soil Carbon
RCPs
MPI-MTE
CLM4.5
Biogeochemical Cycles

ABSTRACT

Atmospheric CO_2 has been dramatically increasing since beginning of the industrial time (i.e. 1860), being one of the main driver for climate change at regional and global level. The change in CO_2 concentration in the atmosphere, together with that of temperature, precipitation and/or so radiation, can influence the biogeochemical cycles in all ecosystems. In this study, we investigate the combined effect of CO_2 concentration and six climate variables on carbon uptake, i.e., gross primary production (GPP) and carbon storage, i.e, soil carbon (SoilC) in terrestrial biosphere by using the Community Land Model (CLM vers. 4.5) and evaluate the model's results against available observation data. We also analysed the change in carbon uptake and storage under a 2°C global mean warming. Results show that the model performed reasonably well for GPP and SoilC at pan-European scale. We also found a positive correlation between GPP, precipitation and surface wind, and a negative correlation between GPP and surface downwelling longwave radiation (rlds). Under a 2°C global warming, GPP and SoilC show an increase, an average, of about 20%, and 5% at pan-European scale, respectively. However, our results indicate that CLM4.5 may need improvements particularly in carbon-nitrogen interaction and carbon accumulation in soil.

Practical Implications

Modelling climate change impacts on carbon uptake and storage capacity of terrestrial biosphere has been an essential research field since monitoring of drastic increase of atmospheric CO_2 due to anthropogenic activities. An alteration in land cover and/or biome types influences particularly the biogeochemical cycles (e.g. carbon and nitrogen cycles) of the terrestrial biosphere and in turn, affect to the carbon sink/source capability of the terrestrial ecosystems. To understand, identify and illustrate the impact of climate change on the sink/source ratio in vegetated regions at pan-European scale, in the study we used a model that correctly simulates the essential biochemical processes and the interactions between processes at high resolution,namely, the CLM4.5.

The results of this study suggest the following practical implications:

- The gross primary productivity (i.e. carbon uptake) (GPP) by autotrophs showed an increase both in observation and modelling studies during last decades. The increase in GPP is mostly related to the impact of both elevated atmospheric CO_2 and climate parameters, which also lead to a fertilization impacts on vegetated regions. Future projections show an increase up to 60% in GPP under climate change, with no change in land cover types and land use at pan-European scale. These results suggest a positive impact of future changes in atmospheric CO_2 and climate on the capacity of terrestrial ecosystem to uptake and store carbon at pan-European scale.
- The comparison of the results when the CLM4.5 was forced by four regional different climate models (RCMs) show minimal differences on the impact of climate change on GPP and soil carbon (SoilC) in terrestrial biosphere at pan-European scale. Although the driving climate from the four RCMs may present large differences, however the response of the biogeochemical cycles to climate change is simulated relatively similarly by CLM4.5. These results highlight that the simulations of CLM 4.5 on the future trajectory of the terrestrial carbon balance are therefore insensitive to the uncertainty in climate model projections.

* Corresponding author at: Iskenderun Technical University, Meydan Mah. 512 Sk., 31230, Iskenderun, Hatay, Turkey.
E-mail address: abdulla.sakalli@iste.edu.tr (A. Sakalli).

http://dx.doi.org/10.1016/j.cliser.2017.03.006
2405-8807/

- Under Climate change model results show a generally uniform growth of GPP across all Europe. On the contrary, the change in SoilC is more heterogeneous, showing almost no change over the Alps, Middle Europe, and Scandinavia, and small increase over France Spain, and UK.
- In general, the carbon biogeochemical cycle and thus the carbon uptake and storage capacity of European vegetated areas will be influenced by global warming up to 2°C in the future. We highly recommend investigating the effect of global warming up to 1°C and 1.5°C to see expected differences between the time periods to make more efficient risk analysis and emergency guide.

1. Introduction

During the Conference of the Parties in Paris (CoP21), a historical agreement was reached to limit the global mean temperature increase since 1860 (pre-industrial) time below 2°C. It is well known that the ecosystems can be dramatically altered by changing environmental factors, with CO_2 rising, change in temperature, precipitation, solar radiation and surface wind as main factors affecting biogeochemical cycles (i.e. carbon, nitrogen, water etc.) in the terrestrial biosphere (Betts et al., 1997; Hungate et al., 2007; Wramneby et al., 2010; IPCC et al., 2014). Many studies showed that an increase of CO_2 in the atmosphere is the main factor for the increase of carbon storage in biomass and soil under optimal conditions (i.e. sufficient nitrogen, phosphor, water, temperature etc.).

However, the question about "how is the carbon storage capacity of an ecosystem affected by climate change?" is still open. In the last decade, many studies have been focusing on finding the critical points of impacts of 2°C global mean temperature increase on relevant processes in the biosphere and atmosphere. Numerical models and field studies were used to investigate the carbon uptake and allocation more carefully and in detail for the terrestrial biosphere. The carbon uptake or, in other words, photosynthesis by autotrophic organisms, depends not only on temperature and precipitation but also by surface downwelling long/shortwave radiation, surface wind and humidity in ecosystems (Ryan, 1991; Cox et al., 2000; Hungate et al., 2003; Tang et al., 2010). A change in photosynthesis due to environmental factors lead directly to a change in primary production, total carbon in vegetation, soil (SoilC), and ecosystems.

There are various modelling studies that show the effect of increasing CO_2 and climate change on the carbon uptake and storage in the terrestrial ecosystem (Betts et al., 1997; Tang et al., 2010). For instance, results by Lucht et al. (2006) showed an increase in total vegetation carbon (TotVegC), SoilC, and also in net primary production (NPP) under climate change (i.e. climate simulations from ECHAM5 climate model under SRES-B1 and SRES-A2 emission scenarios). Also in-situ experiments (e.g. Free Air Carbon Dioxide Enrichment (FACE), Open Top Chamber (OTC), etc. detected a change in the amount of total carbon in vegetation, soil and ecosystem (Norby and Zak, 2011; Tollefson, 2013).

Since the soils contain more carbon than the atmosphere and total biomass on land, a change in the carbon storage capacity of the soil, i.e., the carbon source to sink or vice versa, can affect the atmosphere-biosphere interaction enormously (Tollefson, 2013). Furthermore, the carbon sink capacity of the soils in agricultural and degraded areas amounts to ca. 60% of the historic carbon loss (i.e. $\sim$ 80 GtC) (Lal, 2004). Among others, the aspects highlight the importance of understand the effect of climate change on carbon storage capacity of soils. Total soil carbon includes, among others, above- and below-ground live plant components, i.e., leaf, branch, stem and root, dead biomass, i.e., dead wood, ground litter, and soil inorganic carbon. A reduction of the destructive impacts of the change in atmospheric balance on an ecosystems can be achieved either via reducing the greenhouse gasses concentration, especially carbon dioxide (CO_2), methane (CH_4) and nitrous oxides (NO_x) (Pinder et al., 2012; IPCC et al., 2014) in the atmosphere or other environmental pollutant in the terrestrial and aquatic ecosystems (Sellers et al., 1997).

The impact of CO_2 increase in the atmosphere and the consequent climate change on the biogeochemical cycles, is a well known issue in ecology. In particular, the behaviour of carbon storage in soil, and carbon uptake by vegetation under global atmospheric change have been increasingly investigated. To investigate the impact of CO_2 increase and climate change on soil carbon a numerical model that explicitly simulates the biogeochemical cycles of C (carbon) and N (nitrogen) is needed.

In this study, we aim to investigate the possible impacts of both CO_2 increase and climate change, (i.e. change in solar variables, temperature, precipitation, relative humidity and surface wind) on carbon storage of the vegetation, soil and ecosystem as well as on the carbon sink and source locations at the pan-European level.

2. Materials and Methods

For our aims, we used the Community Land Model version 4.5 (CLM4.5) with the component set-up ICLM45CN (i.e. open carbon nitrogen interaction, no fire, a fixed land-use from 2000 with no land-use change). The model is driven by the following atmospheric variables: temperature, precipitation, surface downwelling longwave and shortwave radiation, relative humidity and wind speed at the lowest atmospheric level (i.e. 10 m). First, the model was run for 700+150 years to initialize the carbon pools until reaching a steady-state (see Section 2.2), following Koven et al. (2013).

After the spin-up run, the model was run for 130 years (from 1971 to 2100) forced by the outputs of RCMs from the EURO-CORDEX initiative (Jacob et al., 2014) with horizontal of 0.11 degrees ($\sim$ 12.5 km). Following the protocol of the FP7 IMPACT2C project, we defined the 2°C period as the time when the 30 year average global mean temperature reaches 2°C, compared to the global warming during pre-industrial period 1881–1910. For each RCM, the global warming is determined by the driving GCM (General Circulation Model) (see Table 1) under RCP4.5 (Representative Concentration Pathways +4.5 $\frac{W}{m^2}$) scenario, in which the anthropogenic greenhouse gas (GHG) emissions peak around 2040. Since the GCMs simulations reached the 2°C earliest in 2034 and latest around 2063, we analysed the data for two time periods i.e. past observed from 1971 to 2000 and future projected periods from 2034 to 2063.

We forced CLM4.5 for the past observed and future projected periods with bias corrected climate parameter (Wilcke et al.,

Table 1
The used EURO-CORDEX simulations with RCP4.5 scenario.

driving GCM	RCM
MPI-ESM-LR-r1	CSC-REMO
IPSL-CM5A-MR-r1	IPSL-INERIS-WRF331F
EC-EARTH-r1	KNMI-RACMO22E
EC-EARTH-r12	SMHI-RCA4

Table 2
The used climate variable for atmospheric forcing of the CLM4.5 model.

Code	Variable name as daily mean value (unit)
tas	surface temperature at 2 m (°C)
pr	sum of precipitation (mm)
rlds	Surface Downwelling Longwave Radiation ($\frac{W}{m^2}$)
rsds	Surface Downwelling Shortwave Radiation ($\frac{W}{m^2}$)
huss	Near-Surface Specific Humidity ($\frac{kg}{kg}$)
sfcWind	Near-Surface Wind Speed ($\frac{m}{s}$)

2013). The forcing climate variable, their acronyms and units are presented in the Table 2.

To analyse the uncertainty in the RCMs' simulation of the present climate (1971–2000), we used following equation for the model agreements;

$$Model_{agr} = \frac{Clim(p,yr) - \overline{Clim(p,yr)}}{\overline{Clim(p,yr)}} * 100 \quad (1)$$

where (%), $Clim(p,yr)$ is the annual climate variable (from 1971 to 2000), and $\overline{Clim(p,yr)}$ is the average of each climate variable from the four RCMs and years, respectively.

2.1. Model Description

In CLM4.5, GPP is modelled according to the following Eqs. (2)–(8):

$$GPP = NPP + (M_R + G_R) \quad (2)$$

where M_R and G_R are maintenance growth respiration, respiration. Maintenance respiration is mainly calculated as the sum of carbon fluxes in leaf, fine root, live steam and live root (see Eq. 1).

$$M_R = CF_{leaf} + CF_{froot} + CF_{livestem} + CF_{livecroot} \quad (3)$$

where CF_{leaf}, CF_{froot}, $CF_{livestem}$, and $CF_{livecroot}$ is maintenance respiration costs for leaf, fine root, live stem, and live coarse root, respectively.

Growth respiration is also calculated as 30% of the total carbon in new growth

$$G_R = 0.3 \cdot GPP \quad (4)$$

In its simplest form, GPP is modelled in CLM4.5 by considering the carboxylation as:

$$GPP = min(A_c, A_j, A_p) \quad (5)$$

The RuBP carboxylase (Rubisco) limited rate of carboxylation A_c ($\mu mol\ CO_2 \cdot m^{-2} \cdot s^{-1}$) is

$$A_c = \left\{ \begin{array}{ll} \frac{V_{cmax}(c_i - \Gamma_*)}{c_i + K_c(1+\frac{o_i}{K_o})} & \text{for} C_3 \text{plants} \\ V_{cmax} & \text{for} C_4 \text{plants} \end{array} \right\} c_i - \Gamma_* \geqslant 0. \quad (6)$$

The light limited maximum rate of carboxylation that allows to regenerate RuBP A_j ($\mu mol\ CO_2 \cdot m^{-2} \cdot s^{-1}$) is

$$A_j = \left\{ \begin{array}{ll} \frac{V_{cmax}(c_i - \Gamma_*)}{4c_i + 8\Gamma_*} & \text{for} C_3 \text{plants} \\ \alpha(4.6\theta) & \text{for} C_4 \text{plants} \end{array} \right\} c_i - \Gamma_* \geqslant 0. \quad (7)$$

The product-limited and PEP carboxylase-limited rate of carboxylation for C_3 and C_4 plants A_p ($\mu mol\ CO_2 \cdot m^{-2} \cdot s^{-1}$) is

$$A_p = \left\{ \begin{array}{ll} 3T_p & \text{for} C_3 \text{plants} \\ k_p(\frac{c_i}{P_{atm}}) & \text{for} C_4 \text{plants} \end{array} \right\} \quad (8)$$

In the equations of the carboxylation, c_i is the partial pressure of CO_2 in internal leaf (Pa), O_i is the partial of O_2 (Pa), K_c and K_o are the Michaelis-Menten constants (Pa) for CO_2 and O_2 is the CO_2 compensation point. V_cmax is the maximum rate of C assimilation ($\mu mol \cdot m^{-2} \cdot s^{-1}$). J stands for electron transport rate ($\mu mol \cdot m^{-2} \cdot s^{-1}$), T_p for triose phosphate utilization rate ($\mu mol \cdot m^{-2} \cdot s^{-1}$), is the absorbed photosynthetically active radiation ($W \cdot m^{-2}$) and k_p is the initial slope of C_4 CO_2 response curve. The detailed description of the parameters can be found in the study by (Oleson et al., 2013).

The modelling of GPP, as formalized above, depends on the plant functional type. The version of the model used the 17 plant functional types (PFT) from the study of Lawrence & Chase (2007).

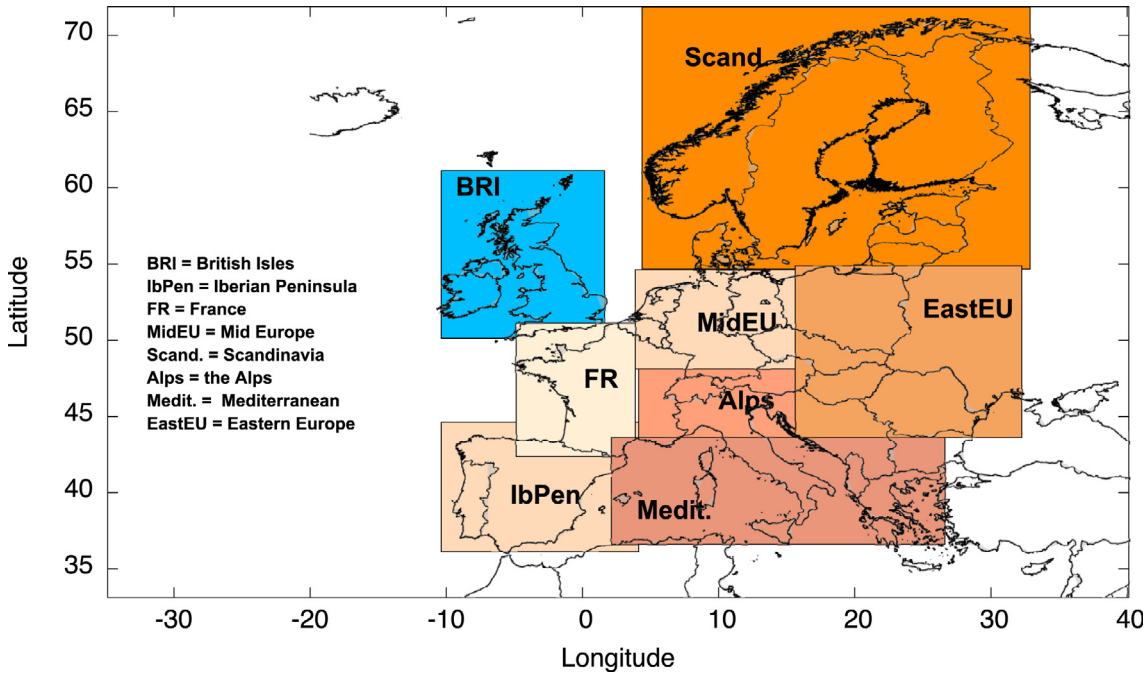

Fig. 1. The division of pan-European domain in to 8 sub-domains by consideration of relative temperature change

2.2. Spining up of the model

The spin-up of the model was performed as it follows: First, the model was run for 700 years, from arbitrary initial conditions, by using the "accelerated decomposition spin-up" to bring the carbon pools (i.e. total vegetation and soil carbon pools) in equilibrium in the terrestrial biosphere. We followed the same methodology from Koven et al. (2013), although, after 700 year the carbon pools reached a steady state, and as a consequence we have not performed complete 1000 year initialization run as suggested by Koven et al. (2013). Subsequently, we run an additional 150 year initialization run with the "accelerated mode" switched on. The accelerated spin-up method needed also atmospheric parameter for forcing the model with atmospheric boundary conditions. We used the required atmospheric boundary conditions from the Table 2. The methodology of generating the EURO-CORDEX climate data was published by Jacob et al. (2014) and Kotlarski et al. (2014). The spin-up run of the model was done with fixed pre-industrial atmospheric CO_2 concentrations and N deposition.

We split the pan-European domain in 8 sub-regions mainly by consideration of change in annual average temperature (adapted from Landgren et al., 2013) (Fig. 2).

2.3. Validation of the model output

For validation of the model results we used in-situ data included empirical up-scaled GPP data from the global network MPI-MTE (Integrating Worldwide CO_2, Water and Energy Flux Measurements) eddy covariance observations by using the methodology from Jung et al. (2009),Jung et al., 2011 and Beer

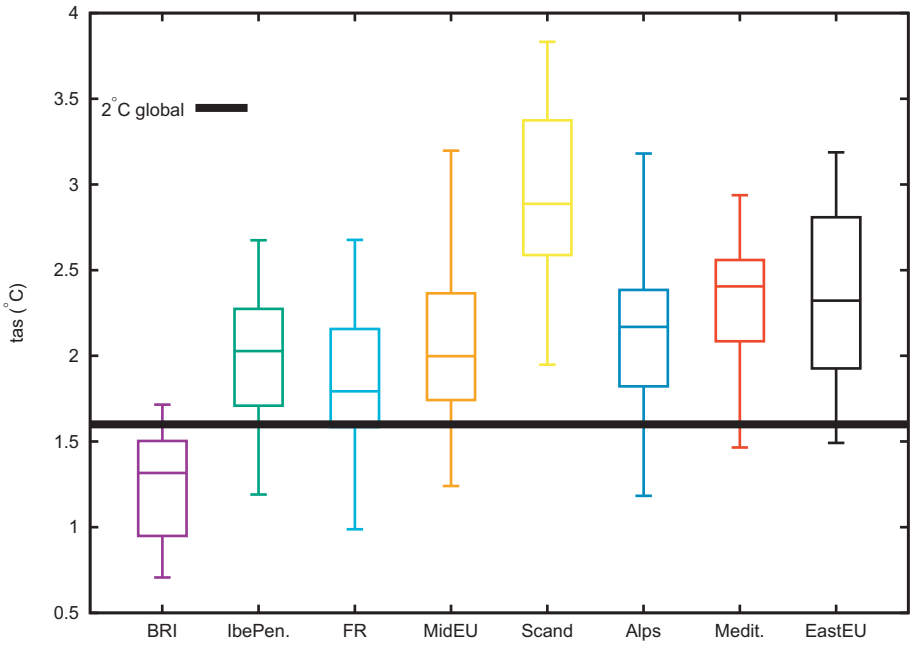

Fig. 2. Future (2034-2063) temperature anomaly relative to the reference period (1971-2000). The middle solid bold line is the average temperature change in pan-European region, when the global average temperature change reached the 2°C

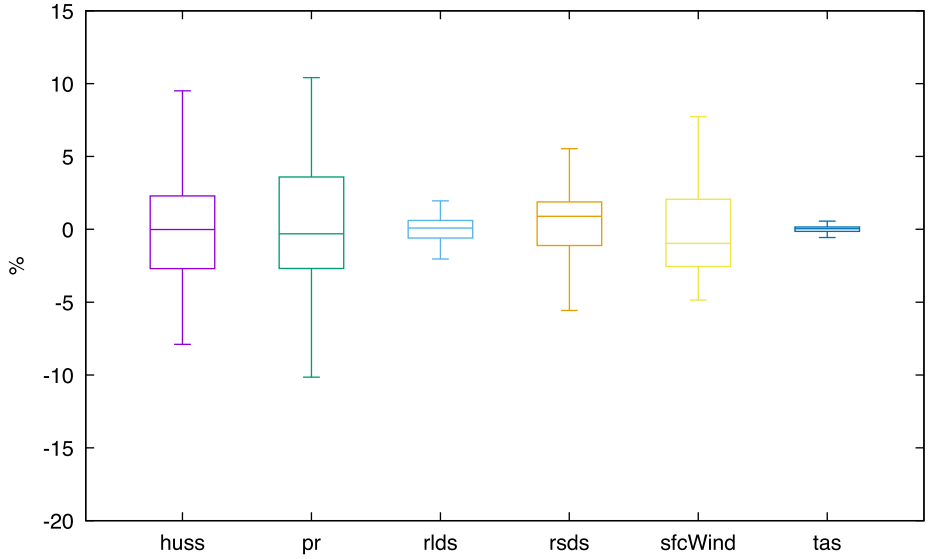

Fig. 3. Agreement in the simulations of the climate variables against the four GCM-RCM at the pan-European level for the reference period (1971-2000)

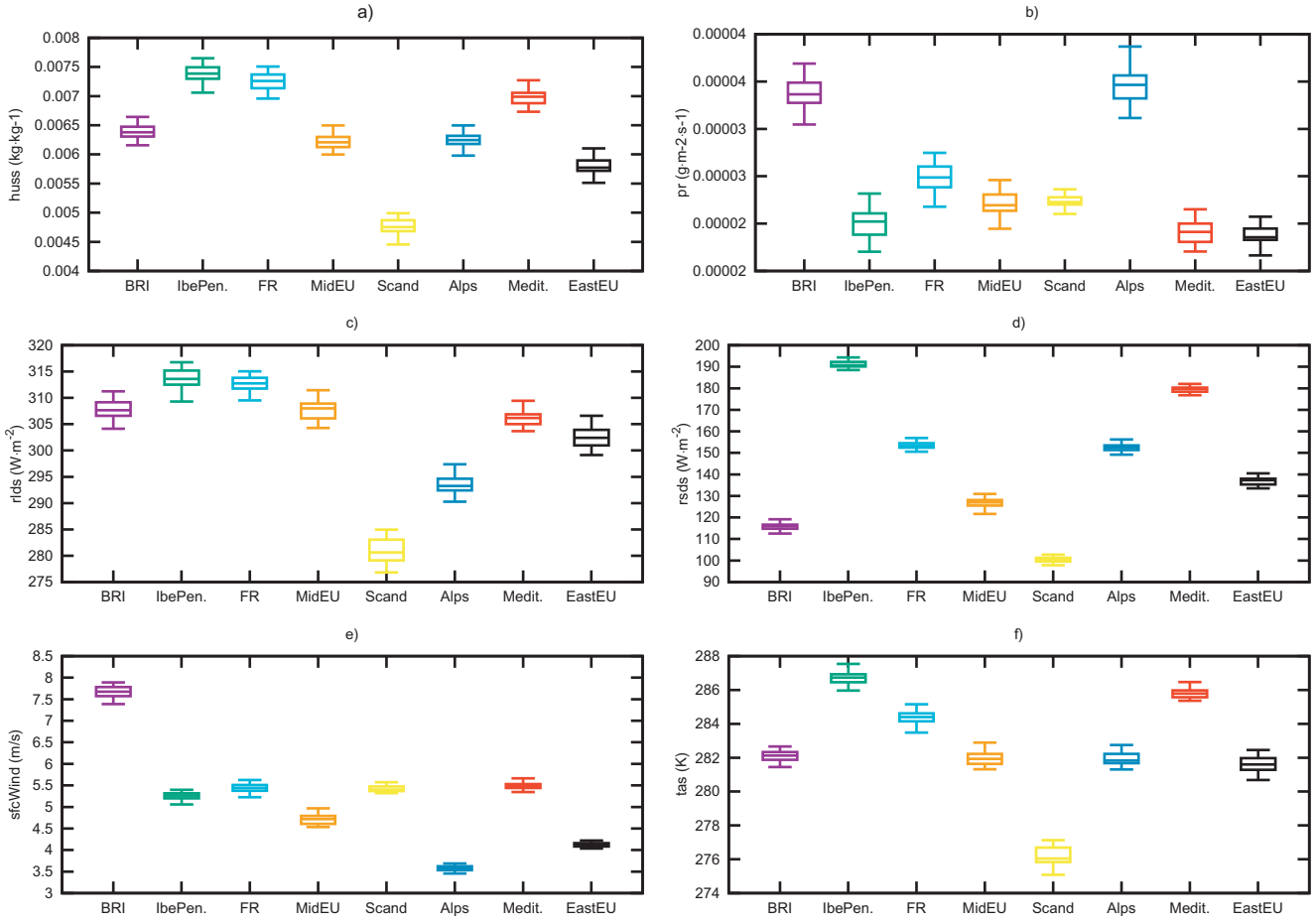

Fig. 4. RCM's uncertainty for the used climate variable in the 8 sub-regions

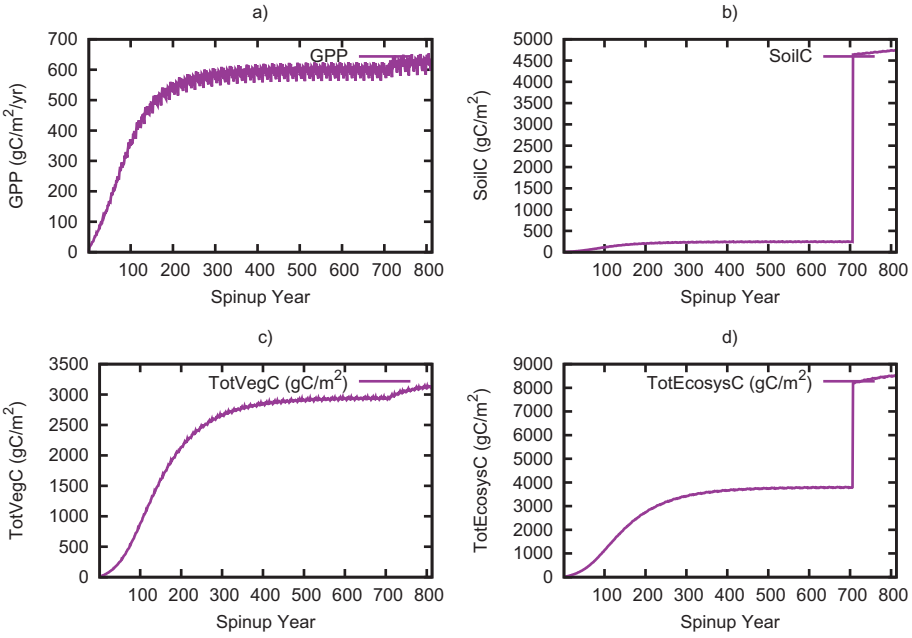

Fig. 5. The relevant pools and flux in the terrestrial biosphere by consideration of a spin-up run by CLM4.5

et al. (2010), and soil carbon from the Harmonized World Soil Database (HWSD version 1.2) (FAO/IIASA/ISRIC/ISSCAS/JRC, xxxx). Both data bases are commonly used and include also long term observation and calibrated data for GPP, SoilC, respectively. The GPP database included data from 1982 up to 2005. To compare modelled and observed GPP, we used therefore the com-

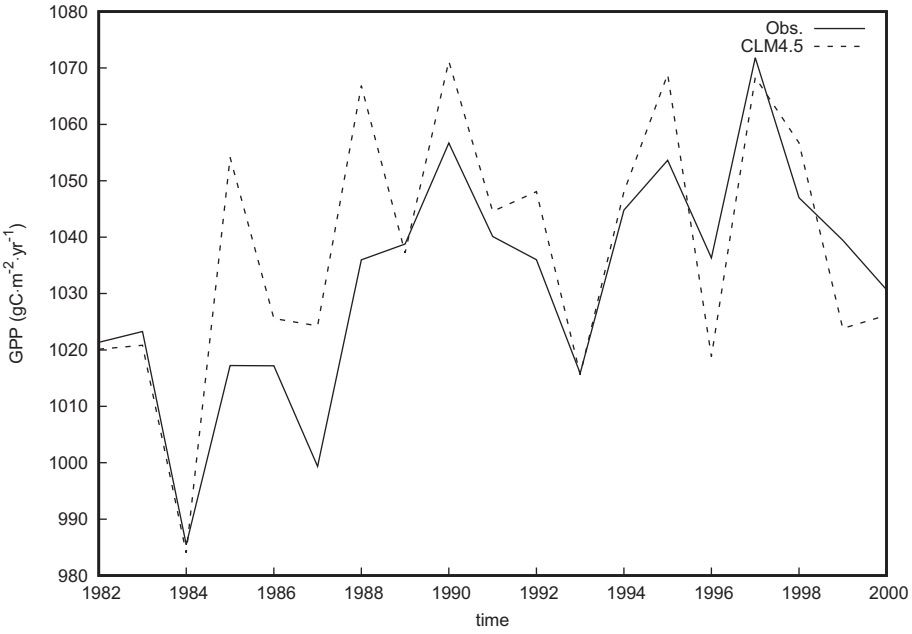

Fig. 6. Comparison of the ensamble mean of modelled GPP by CLM4.5 with the observed GPP by Jung et al. (2011) over the entire pan-European domain

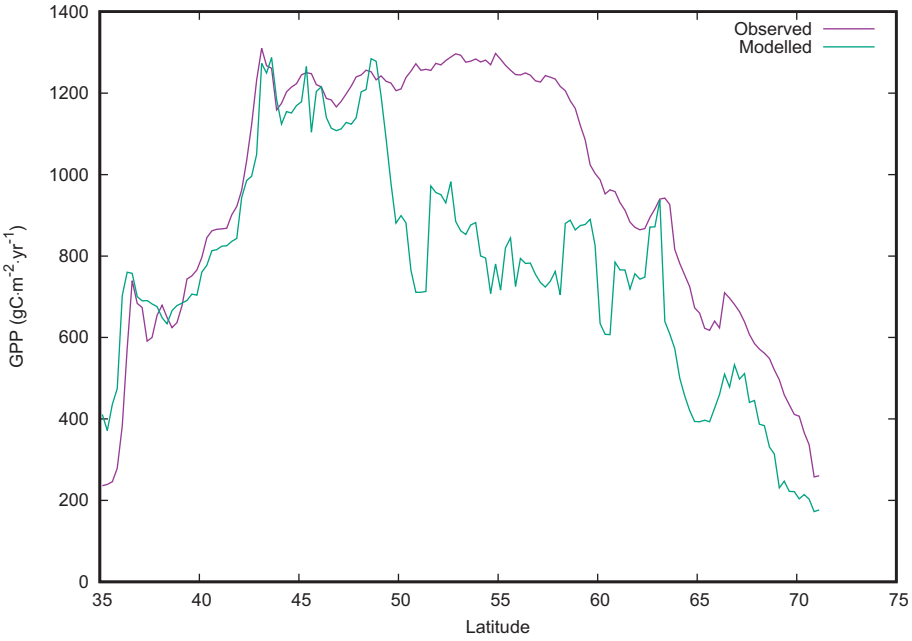

Fig. 7. Comparison of the zonal mean of the time average modelled GPP by CLM4.5 (1982-2000) with the zonal mean of time average observed GPP by Jung et al. (2011)

mon period 1982 to 2000. The HWSD was up-scaled to the 25x25 km grid resolution by using bilinear interpolation, for the origin 1 km resolution by using Climate Data Operators (CDO) (CDO, 2015).

3. Results

3.1. Climate variables

Fig. 2 shows the temperature increase of the four RCMs, a 2°C global warming over the 8 sub-regions. The bold black line in the figure showed the value of the average temperature change (1.6°C) in pan-European region, when the global average temperature change reached the 2°C. The figure shows that most of the regions would become warmer than the global average, with the British Isles being an exception. France shows a warming quite close in median to the global value. It is noteworthy that most of the regions in Europe would exceed 2°C warming before the global average was reached.

To check the agreement of the climate models at pan-European scale, the whisker plot of models' agreement for each climate variable (Eq. 1) is shown in Fig. 3. The figure presents the distribution of the agreement values (N=120, 4 model and 30 years). The highest agreement found for temperature (tas) and longwave radiation (rlds). With a deviation for all annual values (from 1971 to 2000) of around 3% (i.e. from -1.5% to 1.5%) and 4% (from -2% to 2%), respec-

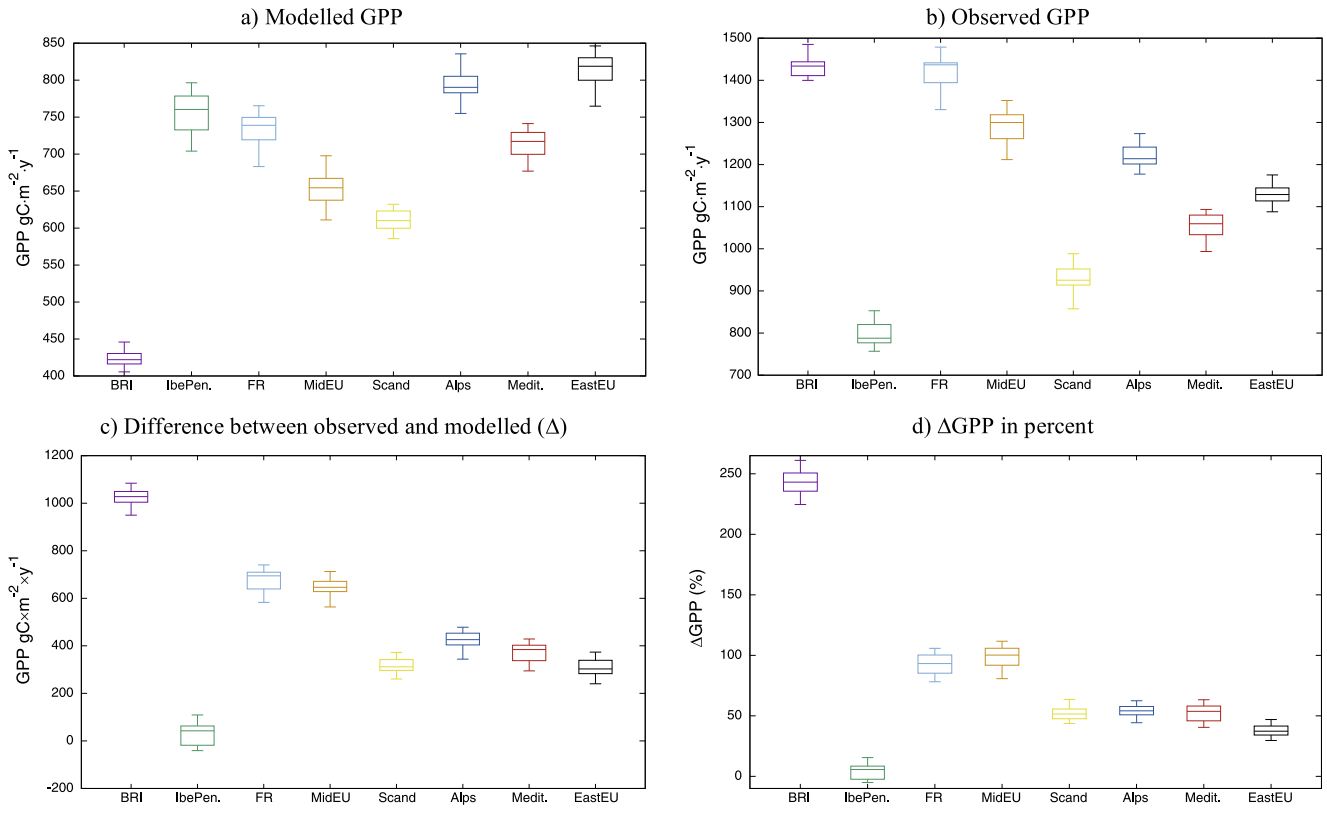

Fig. 8. Comparison of the ensemble mean of modelled GPP by CLM4.5 with the observed GPP by Jung et al. (2011) over the 8 sub-regions of pan-European domain

tively, whereas for precipitation and humidity the agreement is lower, with a deviation up to 20%.

The analysis of the models' uncertainty over the different sub-regions is shown in Fig. 5. The range of the distribution (i.e. difference between maximum value and minimum value) of the climate values are quite similar for most of the climate variable and sub-domains. But the ranges of precipitation (pr) and rlds show most differences between the sub-domains (e.g. BRI and Alps) (see Fig. 5-b).

3.2. Spin-up runs

In Fig. 1, the temporal evolution of the spatial mean (pan-European domain) of relevant carbon pools (i.e. soil carbon, total vegetation and ecosystem carbon) and fluxes (i.e. gross primary production) of the spin-up run is shown. The non-accelerated stage of the spin-up run (700 years run) shows that the soil carbon pool reaches the equilibrium after around 200 years (see Fig. 1-b), but the total vegetation and ecosystem carbon pools and the GPP flux needed ca. 350 years to reach the steady state (see Fig. 1-a,c,d). After switching on the accelerated mode of the spin-up run, all the pools and flux needed a further 100 year period to reach equilibrium. Fig. 1 also shows that the soil carbon pool reached the steady state in ca. 4.7 kgC·m^{-2}, the total vegetation carbon in ca. 3.3 kgC·m^{-2}, and total ecosystem carbon in ca. 8.6 kgC·m^{-2}, respectively.

3.3. Validation of CLM4.5 results

3.3.1. Gross Primary Production

To validate the simulation at pan-European scale the gridded (0.5°) estimates of GPP based on FLUXNET data (MPI-MTE database), climate and remote sensing have been used (Jung et al., 2011). In Fig. 6, the comparison of the simulated and observed GPP data are illustrated for the period 1982–2000. Within the period, the model shows a fairly good agreement with the FLUXNET data with just small biases on few modelled years (e.g. 1985 and 1988).

Fig. 7 shows the difference between zonally averaged observed and modelled GPP over the time period from 1982 to 2000. The model performs quite well at low (35-48°) and high latitude (65-70°), but largely underestimates GPP at mid-latitude (48-60°), where a bias of approx. 400-500 gC·m^{-2}· yr^{-1} (∼ 50%) is found.

Fig. 8 shows the comparison of modelled and observed GPP averaged over the the 8-subdomains. the range (whiskers), 25/75th percentile and median of ensemble means of CLM4.5 runs for GPP in 8 sub-domain of pan-European domain between 1982 and 2000. On Fig. 8-upper-left the distribution of GPP in 8 sub-domains has shown for the time range from 1982 to 2000. It is to see that the model simulated the lowest mean GPP (∼ 430 gC·m^{-2}· yr^{-1}) in the sub-domain 1 (on the British Island) and the highest mean GPP (∼ 820 gC·m^{-2}· yr^{-1}) in the sub-domain 8 (East Europe).

Comparing GPP time evolution for the present and future climate (2°C warming) we note an increase of averaged 50 to 200 gC·m^{-2}· yr^{-1} in all sub-domains (Fig. 9). The lowest increments are simulated in BRI and the highest in eastern Europe.

Comparing the observed GPP with the ensemble mean of results of the four model runs shows quite similar pattern at pan-European scale (see Fig. 10 a,b). In general, GPP is underestimated by CLM4.5 apart from Spain (see Fig. 10 c and d). The highest value for GPP (∼1400 gC·m^{-2}· yr^{-1}) is simulated over temperate climate zones with the PFT "broadleaf deciduous forest" (see Fig. 10-a). In comparison, the up-scaled MPI-MTE database shows the highest GPP (∼1800 gC·m^{-2}· yr^{-1}) value in temperate climate zone with broadleaf deciduous and needleleaf evergreen forests (Fig. 10-b). The largest differences between modelled and observed GPP (approx. 70%) can be noted in temperate climate zone with

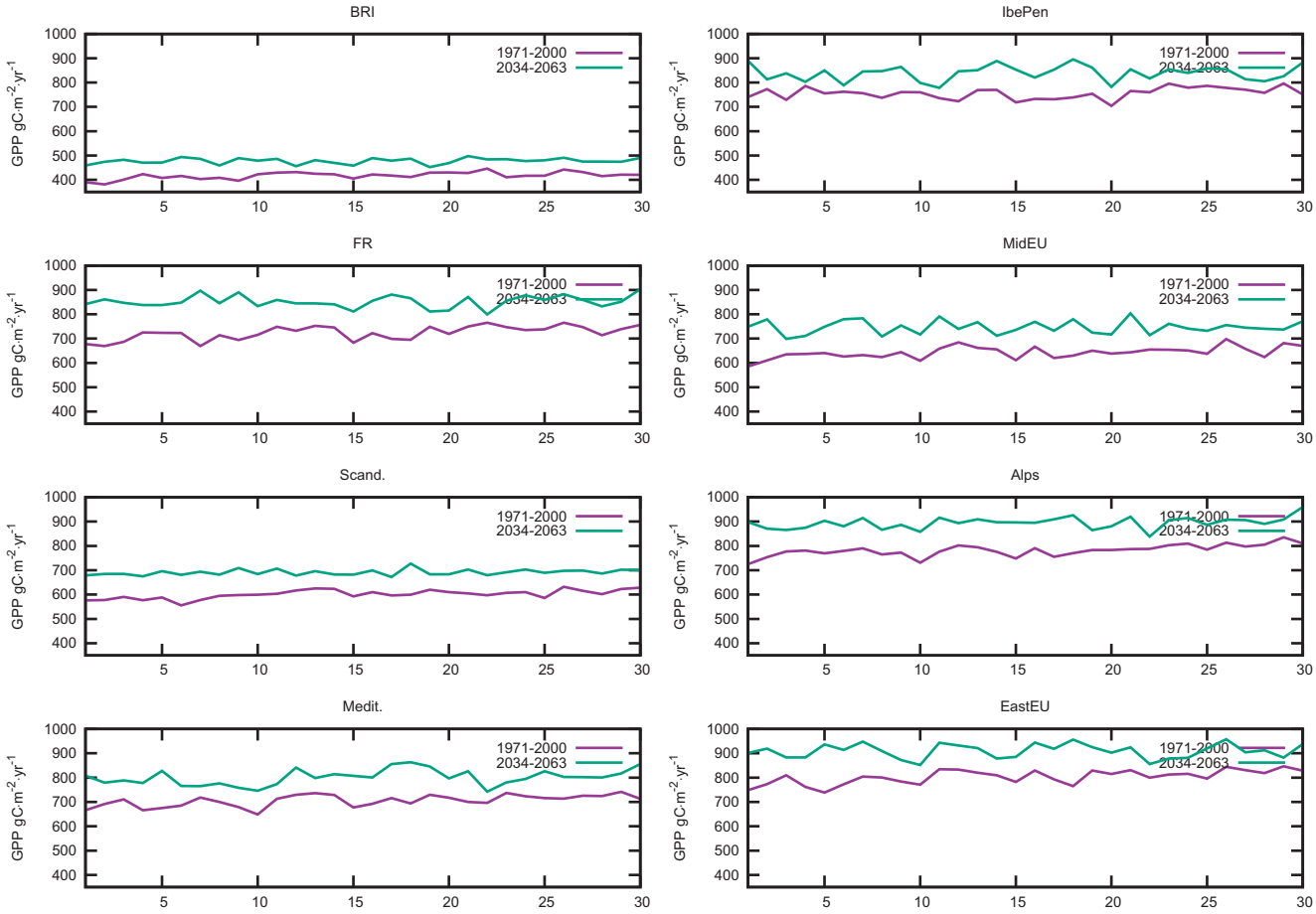

Fig. 9. Comparison of the yearly evolution of the modelled GPP under present and future climate for the 8 sub-regions

broadleaf deciduous forest and crop lands, especially over Great Britain, France and Germany (Fig. 10-d).

3.3.2. Soil Carbon

For validation of soil carbon results by CLM4.5, we compared the modelled soil carbon with soil carbon data from Harmonized World Soil Database (HWSD). In Fig. 11, the modelled, observed and differences between them were presented. Fig. 11-a shows the distribution of modelled soil carbon (SoilC) on pan-European region. The highest SoilC values (>10 kgC·m^{-2}) is modelled over eastern Europe, the Alps and some region of Mediterranean sub-domains. Generally, over FR, Scand, MidEU and IbPen sub-domains, CLM4.5 simulated SoilC less than 6 kgC·m^{-2}. The HWSD database's soil carbon content was converted from percent by weight to weight by area (FAO/IIASA/ISRIC/ISSCAS/JRC, xxxx). In the data base, the soil carbon was estimated higher than 7.5 kgC·m^{-2} in most of the pan-European domain (Fig. 11-b). The amount of soil carbon is especially high (>25 kgC·m^{-2}) in Scandinavia and northern BRI sub-domains. The difference between modelled and observed is plotted in Fig. 11-c and -d. The figures shows a quite large underestimation of SoilC in most of the regions by CLM4.5. Particularly, the difference was very high (>5 kgC·m^{-2} or >250%) in Scandinavia, BRI, northern MidEU along the North Sea coast, and eastern EastEU along the Black Sea and Balkan mountains coast.

The zonal mean of soil carbon is presented in Fig. 12 for modelled and observed data on pan-European domain. The figure shows that the difference between the modelled and observed soil carbon increases with latitude, reaching to maximum between latitude 65° and 70° (ca. 20 kgC·m^{-2}), which is five times higher than the modelled soil carbon. In addition, the time evolution of SoilC zonal gradient of the model is quite different from the soil carbon content of the HWSD database (see Fig. 12). The HWSD database shows highest value of SoilC at high latitudes, while CLM4.5 simulates the lowest value of SoilC in that regions. Also, the value of SoilC for the two 30 year periods (reference and future) is presented in Fig. 13. The figure displays that the soil carbon pool in all sub-domains is slightly effected by climate change in the future.

3.4. Projection of GPP and SoilC by the model

In Fig. 14 we plot the modelled spatial distribution of GPP by CLM4.5 on pan-European domain for the reference (Fig. 14 and future period (Fig. 14-b). The highest values of GPP in the future are located especially over the eastern Europe and Scandinavia, southern France, northern Iberian Peninsula and along the Balkan mountains (Fig. 14(between 1000 and 1400 gC·m^{-2}· yr^{-1}). However, the change in GPP due to global warming in relatively uniform across all Europe (Fig. 14-c) with values usually smaller than 20% (Fig. 14-b). Results with the highest change in GPP (∼50%) are simulated over the Alps, some areas of MidEU, and Scandinavia (Fig. 14-d). The smallest increase (about 2%) in southern IbePen. and along the coasts of Medit. sub-domains (Fig. 14-d).

In this modelling study, we also analysed the change in the soil carbon under climate change. Fig. 15, presents the modelled amounts of soil carbon for the reference, and future projected periods, together with the differences between the two periods. Results show an increase of SoilC due to global warming mainly in western Europe (Fig. 15-c), with the highest increase (∼20%) projected over the Alps, in some areas in northern Sweden and about 12% in France (Fig. 15-d).

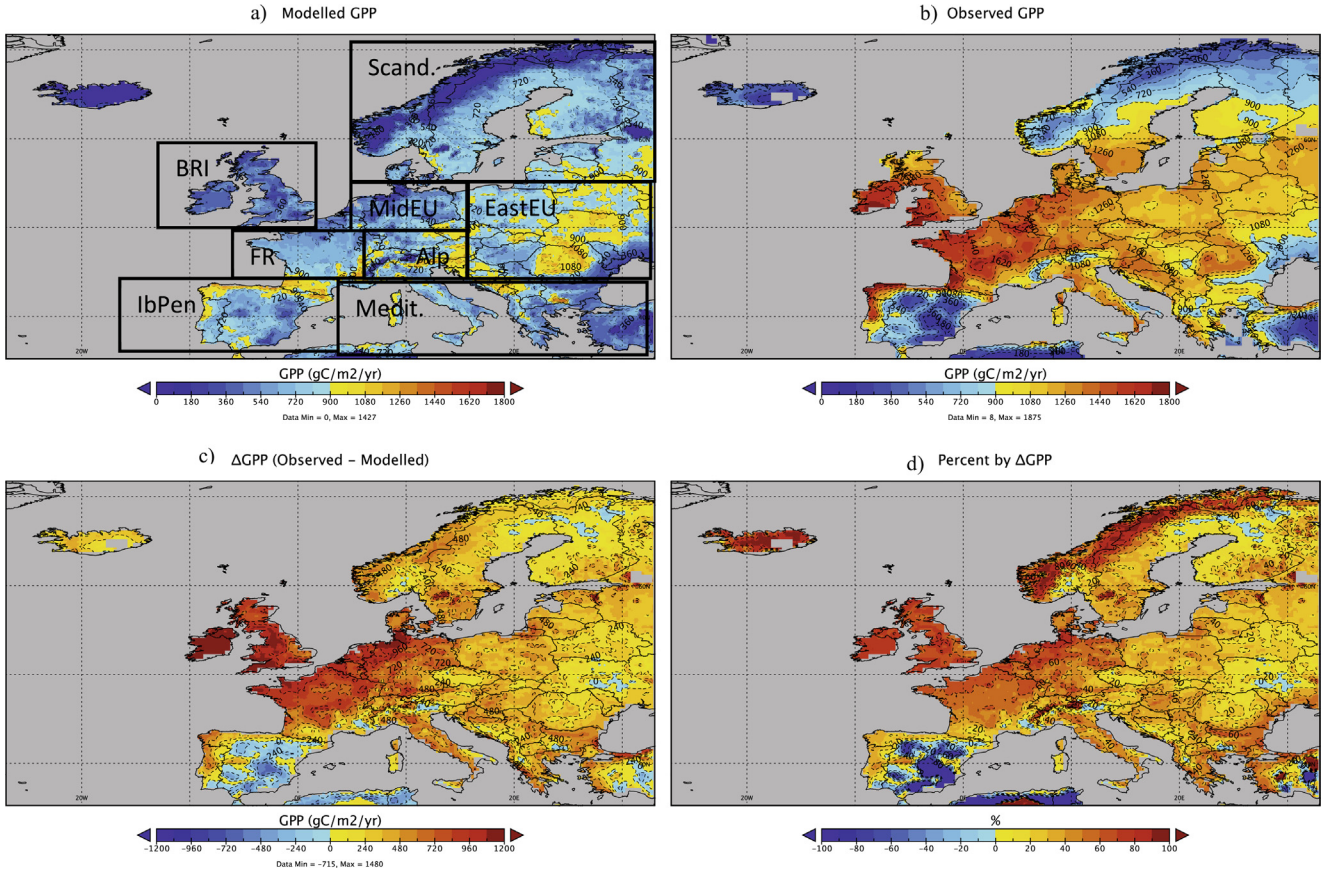

Fig. 10. Spatial distribution of modelled (CLM4.5), observed (Jung et al. (2011) database) and the difference between modelled and observed GPP in pan-European domain for the time average between 1982 and 2000

4. Discussion

Robust modelling of terrestrial GPP is essential to investigate the recent and future trends of the CO2 uptake in different ecosystems and biomasses. Our results show that CLM 4.5 underestimate GPP when compared with observation-driven estimates. This underestimation may be related to the uncertainty arising from the model spin-up. The reason of that could be either the start the model from initial data which were in equilibrium at a different value, a missing/false parameter settings for photosynthesis in the model.

Running the model from a pseudo-equilibrium state of the system can certainly affect the value of variables related to the C pools, that are particularly sensitive to the initialisation assumptions. Koven et al. (2013) published result about the spinning-up techniques for CLM4.0 (Community Land Model version 4.0), and showed that GPP reaches the equilibrium around 800 $gC{\cdot}m^{-2}{\cdot}\ yr^{-1}$ on global average. In our study, GPP reached the steady state at approx. 650 $gC{\cdot}m^{-2}{\cdot}\ yr^{-1}$ on pan-European domain. These differences could be due to i) the spatial resolution, ii) the climate forcing and iii) the model version.

A comparison of the modelled GPP with the up-scaled GPP data of the MPI-MTE database by Jung et al. (2011) showed quite good results in zonal average with some biases (ca. 20-60 $gC{\cdot}m^{-2}{\cdot}\ yr^{-1}$). Also, Bonan et al. (2011) published similar results for the comparison of CLM4.0 zonal average of annual GPP with observed data from MPI-MTE database. Although they found results similar to our at high latitudes, CLM4.0 overestimated the GPP in mid-latitude (Bonan et al., 2011). Beer et al. (2010) also compared zonal means of simulated (by CLM4.5) and observed (FLUXNET) GPP at global level. They showed that CLM4.5 performs quite well at latitudes between 30-40° and 50-60°, but it also shows an underestimation in the latitude range 40-50° and 60-70° (Beer et al., 2010). The differences between the results of this study and those by Bonan et al. (2011) was probably due to the climate forcing and CLM version (i.e. CLM4.0 instead CLM4.5 was used). Therefore, it is possible that GPP is highly depending on the model version and forcing climate. Unlike the correlation at zonal average, the spatial distribution of the observed and modelled GPP displays qiuite different results especially at high latitude (e.g. in BRI and Scand. sub-domains) and high altitude (e.g. in the Alps sub-domain).

Although, the observed and modelled GPP shows similar pattern, there is still quite large difference (up to 80%) between the observed and modelled GPP in the high latitude (i.e. especially between 48° and 60°) that is generally caused by a miss-setting of nitrogen carbon interaction in the model. Houlton et al. (2008),Esser et al. (2011), Zhang et al. (2011), and Zaehle, S (2013) showed that the carbon uptake and storage by plants is highly limited by nitrogen availability in ecosystems. The nitrogen limitation can be up to three times higher than simulation runs with non-nitrogen limitations (Zhang et al., 2011; Zaehle et al., 2013).

On the other hand, the largest disagreement between observed and modelled GPP in the BRI and IbenPen was probably due to the surface wind parameter. Compared to the other climate parameters in the study, surface wind was notable high in these two sub-domains, and therefore probably have highest effectiveness on modelling of GPP by CLM4.5. It is well known that the GPP is highly depend on temperature, precipitation and solar

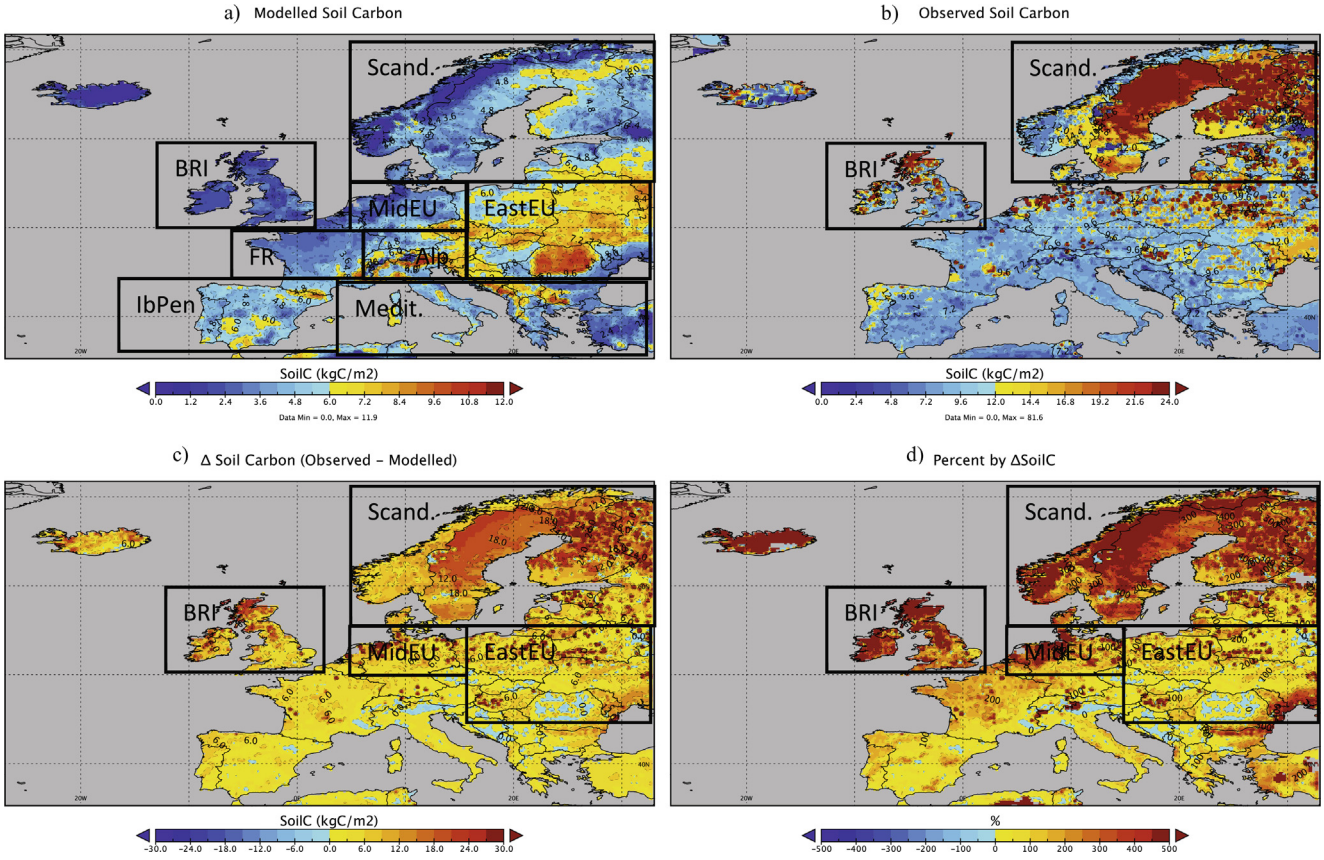

Fig. 11. Spatial distribution of modelled (CLM4.5) and observed (HWSD) SoilC in pan-European domain

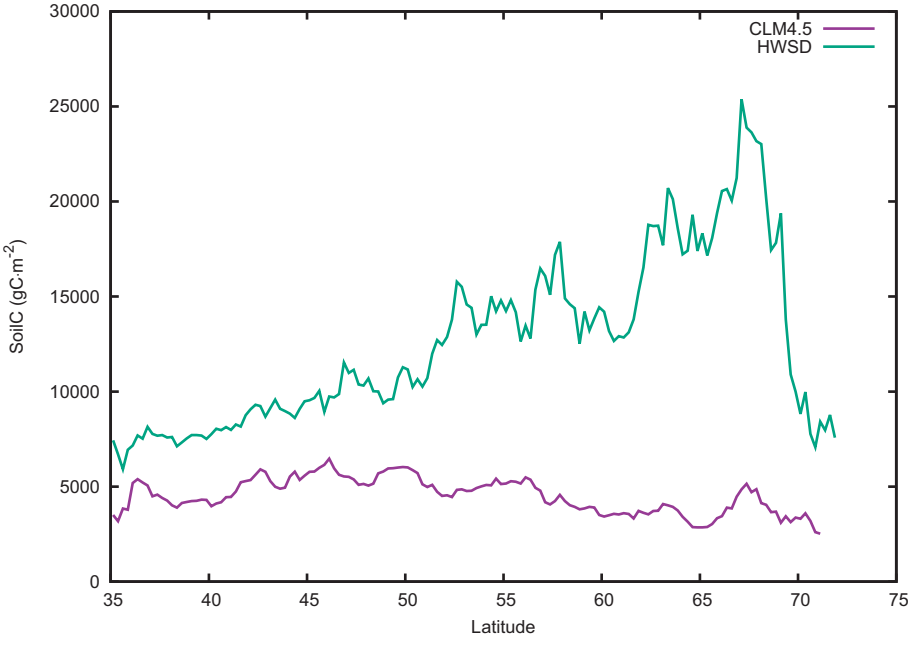

Fig. 12. Comparison of the zonal mean of modelled and observed (HWSD database) SoilC

radiation (Lieth et al., 1975; Turner et al., 2003; Thomey et al., 2011; Pan et al., 2014; Barman et al., 2014; Rambal et al., 2014). Although, there are various studies about the effect of surface wind on gross primary production in aquatic ecosystems, we could not find accurate studies about the surface wind impacts on GPP modelling in terrestrial biosphere (Stanley et al., 2010; Cloern et al., 2014). The multi-variable correlation analysis by Pearson correlation method shows also a significant correlation between surface wind and ΔGPP (future projected period – past observed period) (see Table 3). Surface wind is certainly a very

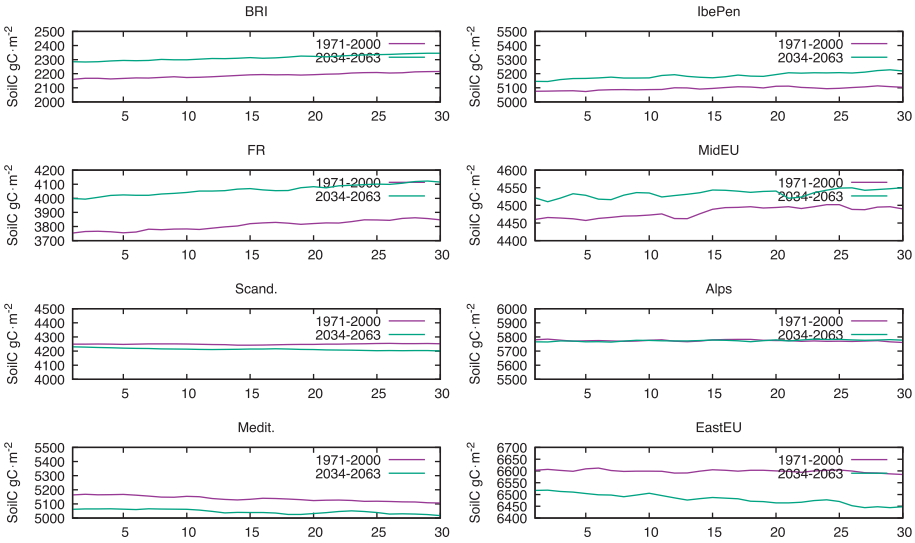

Fig. 13. Comparison of the change in ensemble mean of modelled SoilC by CLM4.5 in 8 sub-domain of pan-European domain and 30 years periods (1971-2000 and 2034-2063)

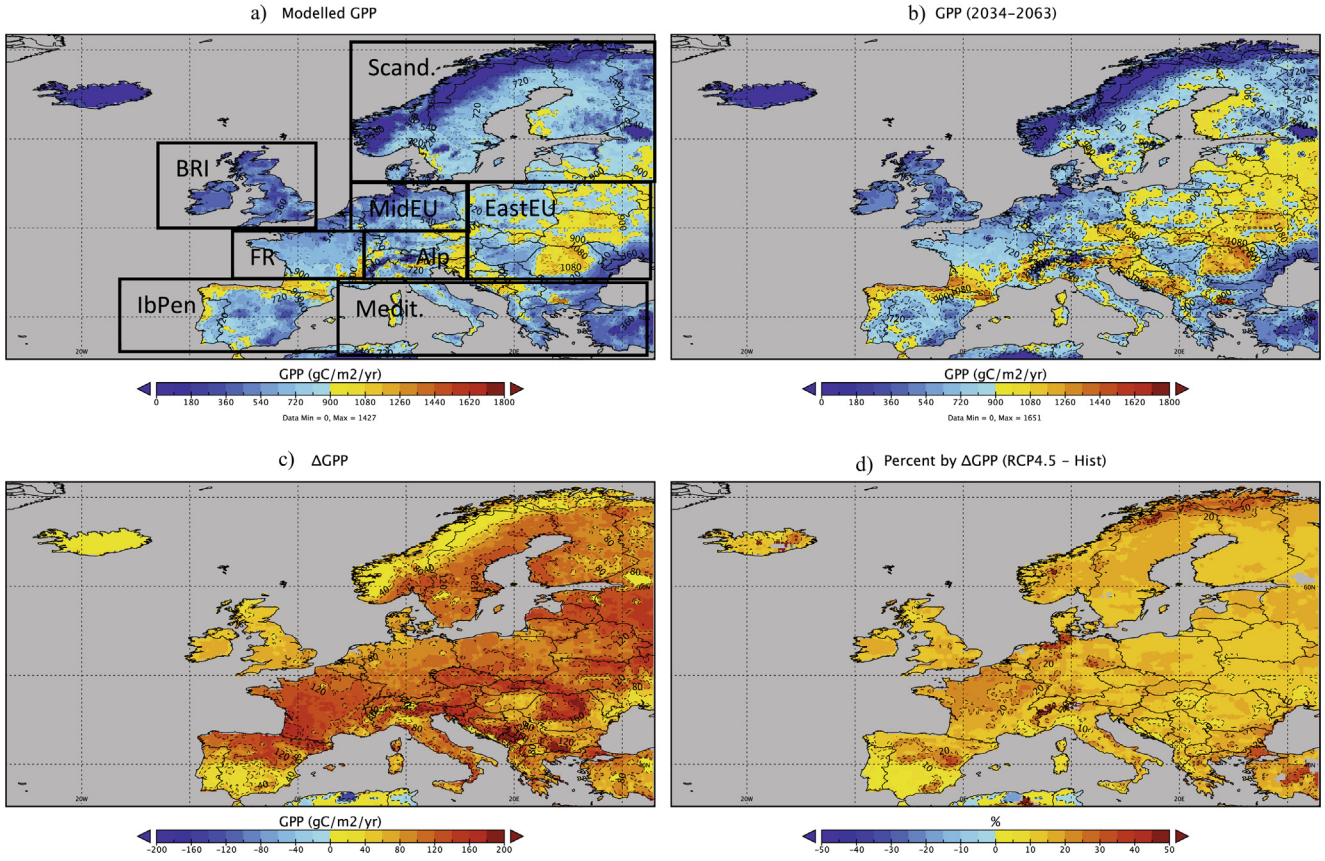

Fig. 14. Modelled GPP by CLM4.5 for the time average between 1971-2000 (a) and 2034-2063 (b), the absolute difference between two periods (c) and the difference in percentage (d)

important parameter for photosynthesis due to effect of saturation of boundary layer of plant leaves (Zelitch et al., 1971). High wind speed ultimately: (i) increase CO2 concentration close to the leaf surface, (ii) reduce heat temperature, (iii) increase transpirations. These processes can affect GPP at certain level. It is an important point to think about making GPP modelling depending also on surface wind.

GPP is projected to an increase under a 2°C global warming, about 20% in most of the regions of Europe, and just about 2% in southern IbePen., and along the coasts of Medit. sub-domains. This shows that GPP over dry regions as IbePen. and Medit. sub-domains will be less effected by climate change than over temperate and boreal regions in Europe. The lower increase of GPP in arid regions is simply due to the increase aridity in area where GPP is

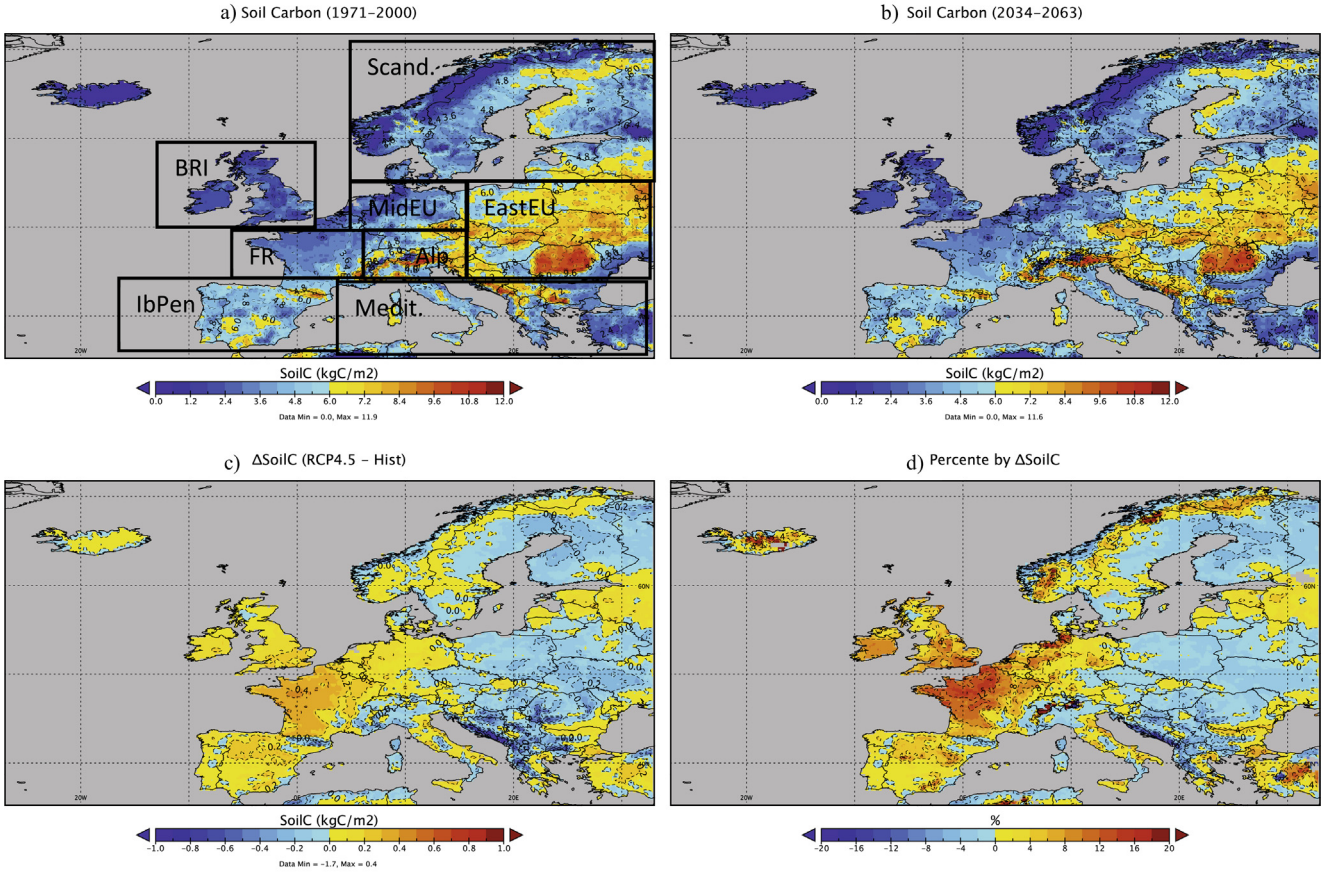

Fig. 15. Modelled SoilC by CLM4.5 for the time average between 1971-2000 (a) and 2034-2063 (b), the absolute difference between two periods (c) and the difference in percentage (d)

Table 3
Correlation coefficient between modelled GPP and used climate parameter by Pearson Correlation Sig. (2 tailed) with 152 sample

	GPP	huss	pr	rlds	rsds	sfcWind	tas
GPP	1						
huss	0.009	1					
pr	0.497**	-0.033	1				
rlds	0.186*	0.875**	-0.143	1			
rsds	-0.504**	0.821**	-0.299*	0.579**	1		
sfcWind	0.582**	0.141	0.229**	0.257**	-0.237**	1	
tas	-0,133	0.962**	-0.184*	0.866**	0.894**	0.051	1

* Correlation is significant at the 0.05 level (2-tailed)
** Correlation is significant at the 0.01 level (2-tailed)

already limited by water availability. This is one of the main outcomes of this modelling study.

Soil carbon plays a key role for carbon sink and source in terrestrial biosphere, and in addition widely accepted that carbon content of the soil improves the physical and chemical properties of the soils. In general, CLM4.5 simulates soil carbon with values closes to the observed over in temperate and Mediterranean regions, but it performs less satisfactory in boreal, alpine and coastal ecosystems. One of the problems in modelled soil organic carbon modelling in non-nitrogen limited ecosystems is related to the mis-parametrisation of the GPP in the model, which leads to less carbon allocation in the soil.

On the other hand, the zonal mean of soil carbon showed a tendency of the model's bias to increase with latitude, with the largest discrepancy ($\sim$ 20 kgC·m^{-2}) between the latitudes 65° and 70°. The HWSD database shows largest values SoilC at high latitudes, while CLM4.5 simulated the lowest soil carbon in that region. When we monitored the change of soil carbon over 30 years periods (i.e. both reference and future), results show that the soil carbon pool in all sub-domains is very slightly effected by climate change. It is well known that in the high latitude the soil has a large carbon stock but small fluxes (Beer et al., 2010). Also a study from Reich et al. (2002), presenting the results of the interannual variability of soil respiration flux at global scale, concluded that the soil respiration

flux had a minimal change in the high latitudes for the study period from 1980 to 1994. Esser et al. (2011) have also reported similar problems about the modelling of the soil organic carbon in non-nitrogen limited regions, over those regions, the model projection is quite questionable. We beelive that the interactions between carbon-nitrogen-phosphor biogechemical cycles have to be more thoroughly investigated especially at high latitudes (Esser et al., 2011; Goll et al., 2012).

Furthermore, future projections show that achieving 2°C global average will influence the soil carbon especially over France and the British Island due to the increase of carbon storage. A consideration of soil respiration and litter production processes could bring more information about the reason(s) of the carbon storage increase in those regions.

5. Conclusion

An accurate study about the modelling of GPP and SoilC help the scientist to identify the range of climate change effect on global or regional level. Although, a model can perform well on global level, on regional level it can have difficulties to match the observation data sets. Principally, CLM4.5 simulates the SoilC and GPP well but obviously with some biases. For improving the modelling of GPP and other relevant processes in the ecosystems, we firstly need to understand the interactions between the biogeochemical cycles (Esser et al., 2011; Goll et al., 2012). Goll et al. (2012) presented critical information about not only the nitrogen and carbon interaction but also phosphorus, carbon and nitrogen interaction and the need about consideration of physical and chemical properties of the biogeochemical cycles. In addition, in modelling studies about the investigation of climate change on biogeochemical cycles not only the common climate parameter (i.e. temperature, precipitation) but also other climate parameter as surface wind should take into account. (See Fig. 4)

Acknowledgements

The research has received funding from the European Communitys Seventh Framework Program (FP7/2007-2013) under grant agreement Nr. 282746 (IMPACT2C).

References

Barman, R., Jain, A., Liang, M., 2014. Climate-driven uncertainties in modeling terrestrial grossprimary production: a site level to global-scale analysis. Global Change Biology 20, 1394–1411. http://dx.doi.org/10.1111/gcb.12474.

Beer, C., Reichstein, M., Tomelleri, E., Ciais, P., Jung, M., Carvalhais, N., Rödenbeck, C., Arain, M.A., Baldocchi, D., Bonan, G.B., Bondeau, A., Cescatti, A., Lasslop, G., Lindroth, A., Lomas, M., Luyssaert, S., Margolis, H., Oleson, K.W., Roupsard, O., Veenendaal, E., Viovy, N., Williams, C., Woodward, F. Ian, Papale, D., 2010. Terrestrial Gross Carbon Dioxide Uptake: Global Distribution and Covariation with Climate. Science 329, 834–838. http://dx.doi.org/10.1126/science.1184984.

Betts, R.A., Cox, P.M., Lee, S.E., Woodward, F.I., 1997. Contrasting physiological and structural vegetation feedbacks in climate change simulations. Nature 387, 796–799.

Bonan, G.B., Lawrence, P.J., Oleson, K.W., Levis, S., Jung, M., Reichstein, M., Lawrence, D.M., Swenson, S.C., 2011. Improving canopy processes in the Community Land Model version 4 (CLM4) using global flux fields empirically inferred from FLUXNET data. Journal of Geophysical Research 116 (G02014), 1–22. http://dx.doi.org/10.1029/2010JG001593.

CDO 2015: Climate Data Operators. Available at: http://www.mpimet.mpg.de/cdo

Cloern, J.E., Foster, S.Q., Kleckner, A.E., 2014. Phytoplankton primary production in the worlds estuarine-coastal ecosystems. Biogeosciences 11, 2477–2501. http://dx.doi.org/10.5194/bg-11-2477-2014.

Cox, P.M., Betts, R.A., Jones, C.D., Spall, S.A., Totterdell, I.J., 2000. Acceleration of global warming due to carbon-cycle feedbacks in a coupled climate model. Nature 408, 184–187. http://dx.doi.org/10.1038/35041539.

Esser, G., Kattge, J., Sakalli, A., 2011. Feedback of carbon and nitrogen cycles enhances carbon sequestration in the terrestrial biosphere. Global Change Biology 17, 819–842. http://dx.doi.org/10.1111/j.1365-2486.2010.02261.x.

Goll, D.S., Brovkin, V., Parida, B.R., Reick, C.H., Kattge, J., Reich, P.B., van Bodegom, P. M., 2012. Niinemets, : Nutrient limitation reduces land carbon uptake in simulations with a model of combined carbon, nitrogen and phosphorus cycling. Biogeosciences 9, 3547–3569. http://dx.doi.org/10.5194/bg-9-3547-2012.

Houlton, B., Wang, Y-P., Vitousek, P.M., Field, C.B., 2008. A unifying framework for dinitrogen fixation in the terrestrial biosphere. Nature 454, 327–331. http://dx.doi.org/10.1038/nature07028.

Hungate, B.A., Dukes, J.S., Shaw, M.R., Luo, Y., Field, C.B., 2003. Nitrogen and climate change. Science 32 (5650), 1512–1513. http://dx.doi.org/10.1126/science.1091390.

Hungate, B.A., Hart, S.C., Selmants, P.C., Boyle, S.I., Gehring, C.A., 2007. Soil responses to management, increased precipitation, and added nitrogen in Ponderosa pine forests. Ecological Applications 17, 1352–1365. http://dx.doi.org/10.1890/06-1187.1.

FAO/IIASA/ISRIC/ISSCAS/JRC.: Harmonized World Soil Database (version 1.2). FAO, Rome, Italy, and IIASA, Laxenburg, Austria.

IPCC, 2014: Climate Change 2014: Impacts, Adaptation, and Vulnerability. Part A: Global and Sectoral Aspects. Contribution of Working Group II to the Fifth Assessment Report of the Intergovernmental Panel on Climate Change [Field, C. B., V.R. Barros, D.J. Dokken, K.J. Mach, M.D. Mastrandrea, T.E. Bilir, M. Chatterjee, K.L. Ebi, Y.O. Estrada, R.C. Genova, B. Girma, E.S. Kissel, A.N. Levy, S. MacCracken, P.R. Mastrandrea, and L.L. White (eds.)]. Cambridge University Press, Cambridge, United Kingdom and New York, NY, USA, 1132 pp.

Jacob, D., Petersen, J., Eggert, B., Alias, A., Christensen, O.B., Bouwer, M.L., Braun, A., Colette, A., Déqué, M., Georgievsk, G., Georgopoulou, E., Gobiet, A., Menut, L., Nikulin, G., Haensler, A., Hempelmann, N., Jones, C., Keuler, K., Kovats, S., Kroener, N., Kotlarski, S., Kriegsmann, A., Martin, E., van Meijgaard, E., Moseley, C., Pfeifer, S., Preuschmann, S., Radermacher, C., Radtke, K., Rechid, D., Rounsevell, M., Samuelsson, P., Somot, S., Soussana, J.-F., Teichmann, C., Valentini, R., Vautard, R., Weber, B., Yiou, P., 2014. EURO-CORDEX: new high-resolution climate change projections for European impact research. Regional Environmental Change 14 (2), 563–578. http://dx.doi.org/10.1007/s10113-013-0499-2.

Jung, M., Reichstein, M., Bondeau, M., 2009. Towards global empirical upscaling of FLUXNET eddy covariance observations: validation of a model tree ensemble approach using a biosphere model. Biogeosciences 6, 2001–2013. http://dx.doi.org/10.5194/bg-6-2001-2009.

Jung, M., Reichstein, M., Margolis, H., Cescatti, A., Richardson, A., Arain, A., Arneth, A., Bernhofer, C., Bonal, D., Chen, J., Gianelle, D., Gobron, N., Kiely, G., Kutsch, W., Lasslop, G., Law, B., Lindroth, A., Merbold, L., Montagnani, L., Moors, E., Papale, D., Sottocornola, M., Vaccari, F.P., Williams, C., 2011. Global patterns of land-atmosphere fluxes of carbon dioxide latent heat and sensible heat derived from eddy covariance satellite and meteorological observations. Journal of Geophysical Research 116, G00J07. http://dx.doi.org/10.1029/2010JG001566.

Kotlarski, S., Keuler, K., Christensen, O.B., Colette, A., Déqué, M., Gobiet, A., Goergen, K., Jacob, D., Lüthi, D., van Meijgaard, E., Nikulin, G., Schär, C., Teichmann, C., Vautard, R., Warrach-Sagi, K., Wulfmeyer, V., 2014. Regional climate modeling on European scales: a joint standard evaluation of the EURO-CORDEX RCM ensemble. Geosci. Model Dev. 7, 1297–1333. http://dx.doi.org/10.5194/gmd-7-1297-2014.

Koven, C.D., Riley, W.J., Subin, Z.M., Tang, J.Y., Torn, M.S., Collins, W.D., Bonan, G.B., Lawrence, D.M., Swenson, S.C., 2013. The effect of vertically resolved soil biogeochemistry and alternate soil C and N models on C dynamics of CLM4. Biogeosciences 10, 7109–7131.

Lal, R., 2004. Soil Carbon Sequestration Impacts on Global Climate Change and Food Security. Science 304, 1623–1627.

Landgren, O., Engen-Skaugen, T., Haugen, J.E. and Kjellström, E., 2013. Evaluation of temperature and precipitation from global and regional climate models, a comparison between different regions in Europe. IMPACT2C Report, Met.NO.

Lieth, H.: Primary Productivity of the Biosphere, H. Lieth, R. H. Whittaker, Springer-Verlag, Berlin, pp. 237–263, 1975.

Lucht, W., Schaphoff, S., Erbrecht, T., Heyder, U., Cramer, W., 2006. Ter- restrial vegetation redistribution and carbon balance under cli- mate change. Carbon Balance and Management 1, 7. http://dx.doi.org/10.1186/1750-0680-1-6.

Norby, R.J., Zak, D.R., 2011. Ecological lessons from Free-Air CO2 Enrichment (FACE) experiments. Annual Review of Ecology, Evolution, and Systematics 42, 181–203. http://dx.doi.org/10.1146/annurev-ecolsys-102209-144647.

Oleson, K. W., Lawrence, D. M., Bonan, G. B., Drewniak, B., Huang, M., Koven, C. D., Levis, S., Li, F., Riley, W. J., Subin, Z. M., Swenson, S. C., Thornton, P. E., Bozbiyik, A., Fisher, R., Kluzek, E., Lamarque, J.-F., Lawrence, P. J., Leung, L. R., Lipscomb, W., Muszala, S., Ricciuto, D. M., Sacks, W., Sun, Y., Tang, J., Yang, Z.-L.: Technical Description of version 4.5 of the Community Land Model (CLM). Ncar Technical Note NCAR/TN-503+STR, National Center for Atmospheric Research, Boulder, CO, 422 pp, 2013. doi: 10.5065/D6RR1W7M.

Pan, S., Tian, H., Dangal, S.R.S., Ouyang, Z., Tao, B., Ren, W., Lu, C., Running, S., 2014. Modeling and Monitoring Terrestrial Primary Production in a Changing Global Environment: Toward a Multiscale Synthesis of Observation and Simulation. Advances in Meteorology 2014, 1–16. http://dx.doi.org/10.1155/2014/965936.

Pinder, R.W., Davidson, E.A., Goodale, C.L., Greaver, T.L., Herric, J.D., Liu, L., 2012. Climate change impacts of US reactive nitrogen. PNAS 109 (20), 7671–7675. http://dx.doi.org/10.1073/pnas.1114243109.

Rambal, S., Lempereur, M., Limousin, J. M., Martin-StPaul, N. K., Ourcival, J. M., and Rodríguez-Calcerrada, J.: How drought severity constrains gross primary production(GPP) and its partitioning among carbon pools in a Quercus ilex

coppice?, Biogeosciences, 11, 6855–6869, doil:10.5194/bg-11-6855-2014, 2014.
Ryan, M.G., 1991. Effects of Climate Change on Plant Respiration. Ecological Applications 1, 157–167. http://dx.doi.org/10.2307/1941808.
Sellers, P.J., Dickinson, R.E., Randall, D.A., Betts, A.K., Hall, F.G., Berry, J.A., Collatz, G. J., Denning, A.S., Mooney, H.A., Nobre, C.A., Sato, N., Field, C.B., Henderson-Sellers, A., 1997. Modeling the exchanges of energy, water, and carbon between continents and the atmosphere. Science 275, 502–509. http://dx.doi.org/10.1126/science.275.5299.502.
Stanley, R.H.R., Kirkpatrick, J.B., Cassar, N., Barnett, B.A., Bender, M.L., 2010. Net community production and gross primary production rates in the western equatorial Pacific. Global Biogeochemical Cycles 24 (GB4001), 1–17. http://dx.doi.org/10.1029/2009GB003651.
Tang, G., Beckage, B., Smith, B., Miller, P. A.: Estimating potential forest NPP, biomass and their climatic sensitivity in New England using a dynamic ecosystem model. Ecosphere, 1(6), art18, 2010.
Thomey, M.L., Collins, S.L., Vargas, R., Johnson, J.E., Brown, R.F., Natvig, D.O., Friggens, M.T., 2011. Effect of precipitation variability on net primary production and soil respiration in a Chihuahuan Desert grassland. Global Change Biology 17, 1505–1515. http://dx.doi.org/10.1111/j.1365-2486.2010.02363.x.
Tollefson, J., 2013. Experiment aims to steep rainforest in carbon dioxide. Sensor-studded plots in the Amazon forest will measure the fertilizing effect of the gas. Nature 496, 405–406. http://dx.doi.org/10.1038/496405a.
Turner, D.P., Ritts, W.D., Cohen, W.B., Gower, S.T., Zhao, M., Running, S.W., Wofsy, S. C., Urbanski, S., Dunn, A.L., Munger, J.W., 2003. Scaling Gross Primary Production (GPP) over boreal and deciduous forest landscapes in support of MODIS GPP product validation. Remote Sensing of Environment 88, 256–270. http://dx.doi.org/10.1016/j.rse.2003.06.005.
Wilcke, R.A.I., Mendlik, T., Gobiet, A., 2013. Multi-variable error correction of regional climate models. Climatic change 120 (4), 871–887. http://dx.doi.org/10.1007/s10584-013-0845-x.
Wramneby, A., Smith, B., Samuelson, P., 2010. Hot spots of vegetation-climate feedbacks under future greenhouse forcing in Europe. Journal of Geophysical Research 115, D21119. http://dx.doi.org/10.1029/2010JD014307.
Zaehle, S.: Terrestrial nitrogen–carbon cycle interactions at the global scale. Philosophical Transactions of the Royal Society, B 368, pp 1–9, 2013. doil: 10.1098/rstb.2013.0125.
Zelitch, Israel, 1971. Photosynthesis, Photorespiration, and Plant Productivity. Academic Press, New York and London.
Zhang, Q., Wang, Y.P., Pitman, A.J., Dai, Y.J., 2011. Limitation of the nitrogen and phosphorus on the terrestrial carbon uptake in the 20th century. Geophysical Research Letters 38 (L22701), 1–5. http://dx.doi.org/10.1029/2011GL049244.